H^{∞} –Tracking Based Adaptive Control for A Class of Multivariable Uncertain Nonlinear Systems using Recurrent CMAC

Chih-Min Lin, *Member, IAENG* , Ming-Hung Lin and Chiu-Hsiung Chen

***Abstract*—A H^{∞}-tracking based adaptive control scheme is proposed for a class of uncertain nonlinear systems. The proposed control system is comprised of a recurrent cerebellar model articulation controller (RCMAC) and a compensation controller. RCMAC is used to mimic an ideal controller, and the parameters of RCMAC are on-line tuned by the derived adaptive laws based on a Lyapunov function. The compensation controller is designed to suppress the influence of approximation error between the ideal controller and RCMAC, and to achieve a robust tracking performance with specified attenuation level. Finally, two uncertain nonlinear systems, a one-link rigid robotic manipulator and a mass-spring-damper mechanical system, are demonstrated to verify the effectiveness of the proposed control scheme.**

***Index Terms*—Adaptive control, recurrent cerebellar model articulation controller (RCMAC), nonlinear systems.**

I. INTRODUCTION

During the past years, many authors have devoted a lot of effort to both theoretical and implementation techniques to handle nonlinear control problem. For multi-input-multi-output (MIMO) nonlinear systems, the control problem is very complicated due to the couplings among various inputs and outputs. By many researchers, different control efforts have been developed from a point of view of dynamic system theory and traditional feedback control. However, these control schemes can be only applied to nonlinear systems whose dynamic functions are exactly known. This is not sufficient for practical control applications, because it is difficult to establish an exactly mathematical model for a large amount of nonlinear systems. To tackle this problem, the adaptive control methodologies based on Lyapunov stability theorem that incorporate the intelligent systems (such as fuzzy system and neural network) have been grown rapidly. A stable adaptive fuzzy control scheme has been developed for controlling the single-input-single-output (SISO) nonlinear systems [27]. By incorporating with sliding-mode control, several adaptive fuzzy sliding-mode control systems have been proposed [11], [16], [18]. Based on the same idea, Hung and Chung presented the self-tuning fuzzy sliding mode control and adaptive neural network-based sliding-mode control for nonlinear systems [9], [10]. Moreover, a number of investigators have proposed the adaptive neural network control techniques for SISO nonlinear plants with unknown nonlinear functions [6], [8], [26]. However, most of these studies did not eliminate the influence of approximation error appropriately so that the favorable tracking performance can not be yielded. For this requirement, the robust bound controller with an estimation law is derived to estimate the approximation error bound so that the approximation error can be compensated [17], [19]. Nevertheless, the estimation law is always a positive value, this even will cause the estimated bound increase to infinity, thus results in the control input eventually being saturated and the system may be unstable. To improve this shortcoming, several adaptive intelligent controllers have been integrated with H^{∞} control technique to achieve intelligent robust control [5], [20], [22], [24]. In these control schemes, the controllers are generally composed of two main components. One is an adaptive control system that is used to approximate an ideal control law. The other is a robust compensator that is designed to attenuate the effect of approximation error to a prescribed level so as to achieve the H^{∞}-tracking performance. Even so, most papers only focused on the single-input single-output control systems. A number of works can be found for nonlinear multiple-input-multiple-output (MIMO) systems based on adaptive control and H^{∞} control techniques. For instance, Chang etc. proposed adaptive H^{∞} control schemes to resolve the tracking control problem of MIMO nonlinear systems [3], [4]. However, these control approaches belong to model-based control schemes that required the partial system model of the control systems. Unfortunately, for a lot of uncertain nonlinear systems, it is difficult to acquire system models in practical control applications. In order to achieve the model-free controller design, some authors presented the adaptive fuzzy controllers that utilized two fuzzy systems to realize optimal

Manuscript received May 19, 2007. The authors would like to acknowledge the financial support in part of the National Science Council of Taiwan, R.O.C. through grant number NSC 94-2213-E-155-010.

Chih-Min Lin is with the Department of Electrical Engineering, Yuan-Ze University Chung-Li, Tao-Yuan, 320, Taiwan, Republic of China (phone: +886-4638800-2418; fax: +886-4639355; e-mail: cml@saturn.yzu.edu.tw).

Ming Hung Lin, is with Department of Electrical Engineering, Yuan-Ze University Chung-Li, Tao-Yuan, 320, Taiwan, Republic of China

Chiu-Hsiung Chen is with Department of Electrical Engineering, Yuan-Ze University Chung-Li, Tao-Yuan, 320, Taiwan, Republic of China

(Advance online publication: 15 August 2007)

control law [2], [14], [23], [24]; thus the nominal part of control plants are not required. But, these control approaches suffer the computational complexity.

Neural network control of nonlinear system has been extensively studied in the past decades. On the neural network structure aspect, cerebellar model articulation controller (CMAC) is classified as a non-fully connected perceptron-like associative memory network with overlapping receptive-fields [1]; and it intends to resolve the fast size-growing problem and the learning difficult in currently available types of neural networks. Comparing to neural networks, CMAC possesses good generalization capability, fast learning ability and simple computation [1], [13]. This network has already been shown that it can approximate a nonlinear function over a domain of interest to any desired accuracy [7], [12], [13]. For the reasons, CMAC have adopted widely for the closed-loop control of complex dynamical systems in recent literatures [15], [19], [21]. However, the major drawback of these CMAC control systems is that their application domain is limited to static problem due to their inherent network structure.

This paper investigates an H^∞-tracking based adaptive control scheme for multiple-input-multiple-output (MIMO) uncertain nonlinear systems. The H^∞-tracking based adaptive control system is comprised of a recurrent cerebellar model articulation controller (RCMAC) and a compensation controller. Since the delayed recurrent feedback is used, RCMAC presents a dynamic network. Thus, it is more suitable for dynamic function approximation. RCMAC is utilized to approximate an ideal controller, and the parameters of RCMAC are on-line tuned by the derived adaptive laws based on a Lyapunov function. From H^∞ control technique, the compensation controller is designed to suppress the influence of approximation error between the ideal controller and RCMAC, so that the desired robust tracking performance can be obtained. Finally, two MIMO nonlinear systems, a one-link rigid robotic manipulator and a mass-spring-damper mechanical system, are demonstrated to verify the effectiveness of the proposed control scheme.

The rest of this paper is organized as follows. Problem formulation is described in Section 2. The design procedures of H^∞-tracking based adaptive control system is described in Section 3. In Section 4, simulation results are provided to validate the effectiveness of the proposed control system. Conclusions are drawn in Section 5.

II. PROBLEM FORMULATION

Consider a class of n-th order multi-input multi-output uncertain nonlinear systems described by the following equation:

$$\boldsymbol{x}^{(n)}(t) = \boldsymbol{f}(\underline{\boldsymbol{x}}(t)) + \boldsymbol{G}(\underline{\boldsymbol{x}}(t))\boldsymbol{u}(t) + \boldsymbol{d}(t) \tag{1}$$

where $\boldsymbol{u}(t) = [u_1(t), u_2(t), \cdots, u_m(t)]^T \in \Re^m$ and $\boldsymbol{x}(t) = [x_1(t), x_2(t), \cdots, x_m(t)]^T \in \Re^m$ denote the control input and state vectors of the system, respectively; in which m is the number of system inputs and outputs; and $\boldsymbol{d}(t) = [d_1(t), d_2(t), \cdots, d_m(t)]^T \in \Re^m$ denotes the unknown but bounded external disturbance. Define $\underline{\boldsymbol{x}}(t) = [\boldsymbol{x}^T(t), \dot{\boldsymbol{x}}^T(t), \cdots, \boldsymbol{x}^{(n-1)T}(t)]^T \in \Re^{mn}$ as the system state vector, and it is assumed to be available for measurement. In addition, $\boldsymbol{f}(\underline{\boldsymbol{x}}(t)) \in \Re^m$ and $\boldsymbol{G}(\underline{\boldsymbol{x}}(t)) \in \Re^{m\times m}$ represent smooth nonlinear uncertain functions and they are assumed to be bounded. Meanwhile, assume that the nonlinear system of Eq. (1) is controllable and $\boldsymbol{G}^{-1}(\underline{\boldsymbol{x}}(t))$ exists for all $\underline{\boldsymbol{x}}(t)$.

When neglecting the modeling uncertainties and external disturbance, the nominal system of Eq. (1) can be obtained as

$$\boldsymbol{x}^{(n)}(t) = \boldsymbol{f}_n(\underline{\boldsymbol{x}}(t)) + \boldsymbol{G}_n(\underline{\boldsymbol{x}}(t))\boldsymbol{u}(t) \tag{2}$$

where $\boldsymbol{f}_n(\underline{\boldsymbol{x}}(t))$ and $\boldsymbol{G}_n(\underline{\boldsymbol{x}}(t))$ are the nominal parts of $\boldsymbol{f}(\underline{\boldsymbol{x}}(t))$ and $\boldsymbol{G}(\underline{\boldsymbol{x}}(t))$, respectively. When the modeling uncertainties and external disturbance exist, the uncertain system of Eq. (1) can be formulated as

$$\begin{aligned}\boldsymbol{x}^{(n)}(t) &= \boldsymbol{f}_n(\underline{\boldsymbol{x}}(t)) + \Delta\boldsymbol{f}(\underline{\boldsymbol{x}}(t)) + [\boldsymbol{G}_n(\underline{\boldsymbol{x}}(t)) + \Delta\boldsymbol{G}(\underline{\boldsymbol{x}}(t))]\boldsymbol{u}(t) + \boldsymbol{d}(t)\\ &= \boldsymbol{f}_n(\underline{\boldsymbol{x}}(t)) + \boldsymbol{G}_n(\underline{\boldsymbol{x}}(t))\boldsymbol{u}(t) + \boldsymbol{n}(\underline{\boldsymbol{x}}(t), t)\end{aligned} \tag{3}$$

where $\Delta\boldsymbol{f}(\underline{\boldsymbol{x}}(t))$ and $\Delta\boldsymbol{G}(\underline{\boldsymbol{x}}(t))$ denote the unknown uncertainties of $\boldsymbol{f}(\underline{\boldsymbol{x}}(t))$ and $\boldsymbol{G}(\underline{\boldsymbol{x}}(t))$, respectively; $\boldsymbol{n}(\underline{\boldsymbol{x}}(t), t)$ referred to as the lumped uncertainty is defined as $\boldsymbol{n}(\underline{\boldsymbol{x}}(t), t) = \Delta\boldsymbol{f}(\underline{\boldsymbol{x}}(t)) + \Delta\boldsymbol{G}(\underline{\boldsymbol{x}}(t))\boldsymbol{u}(t) + \boldsymbol{d}(t)$.

The control objective is to design an H^∞-tracking based adaptive control system such that the system output $\boldsymbol{x}(t)$ can track a desired trajectory $\boldsymbol{x}_d(t)$.

Define the tracking error as

$$\boldsymbol{\varepsilon} \triangleq \boldsymbol{x}_d - \boldsymbol{x} \in \Re^m \tag{4}$$

then the system tracking error vector is defined as

$$\underline{\boldsymbol{\varepsilon}} \triangleq [\varepsilon^T, \dot{\varepsilon}^T, \cdots, \varepsilon^{(n-1)T}]^T \in \Re^{mn} \tag{5}$$

If the nominal functions $\boldsymbol{f}_n(\underline{\boldsymbol{x}}(t))$, $\boldsymbol{G}_n(\underline{\boldsymbol{x}}(t))$ and the lumped uncertainty $\boldsymbol{n}(\underline{\boldsymbol{x}}(t), t)$ can be exactly known, then an ideal controller can be designed as

$$\boldsymbol{u}_{id} = \boldsymbol{G}_n^{-1}(\underline{\boldsymbol{x}}(t))[\boldsymbol{x}_d^{(n)} - \boldsymbol{f}_n(\underline{\boldsymbol{x}}) - \boldsymbol{n}(\underline{\boldsymbol{x}}, t) + \underline{\boldsymbol{L}}^T\underline{\boldsymbol{\varepsilon}}] \tag{6}$$

where $\underline{\boldsymbol{L}} = [\boldsymbol{L}_n, \cdots, \boldsymbol{L}_2, \boldsymbol{L}_1]^T \in \Re^{mn\times m}$ is the feedback gain matrix which contains real numbers.

Substituting the ideal controller Eq. (6) into Eq. (3), gives the error dynamic equation

$$\boldsymbol{\varepsilon}^{(n)} + \underline{\boldsymbol{L}}^T\underline{\boldsymbol{\varepsilon}} = \boldsymbol{0} \tag{7}$$

In Eq. (7), if $\underline{\boldsymbol{L}}$ is chosen to correspond to the coefficients of a Hurwitz polynomials, it implies $\lim_{t\to\infty}\|\underline{\boldsymbol{\varepsilon}}\| = 0$. However, the lumped uncertainty $\boldsymbol{n}(\underline{\boldsymbol{x}}(t), t)$ is generally unknown for practical applications, so that $\boldsymbol{u}_{id}$ in Eq. (6) is unavailable. Thus, an H^∞-tracking based adaptive control system is proposed to achieve trajectory tracking control. In this control system, an RCMAC is used to approximate the ideal controller.

III. H^∞-TRACKING BASED ADAPTIVE CONTROL SYSTEM DESIGN

The block diagram of H^∞-tracking based adaptive control scheme is shown in Fig. 1, where the control system comprises of a recurrent cerebellar model articulation controller (RCMAC) and a compensation controller, i.e.

$$\boldsymbol{u}_{HBAC} = \hat{\boldsymbol{u}}_{RCMAC} + \boldsymbol{u}_H \tag{8}$$

where $\hat{\boldsymbol{u}}_{RCMAC}$ is an RCMAC utilized to approximate the ideal controller $\boldsymbol{u}_{id}$. In this study, the inputs of RCMAC are the tracking error vector shown in Eq. (5) and the outputs of RCMAC are the control efforts so that the input and output numbers of RCMAC are given as $n_a = mn$ and $n_o = m$. $\boldsymbol{u}_H$ is the compensation controller that is designed to suppress the influence of residual approximation error between the ideal controller and RCMAC.

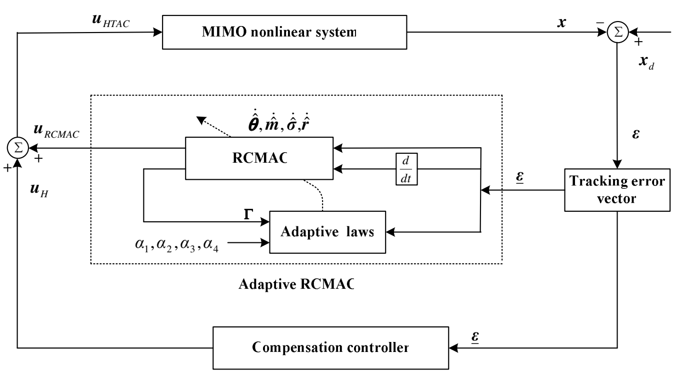

Fig. 1 The block diagram of H^∞-tracking based adaptive control system.

A. RCMAC controller design

In this section, a multi-input multi-output RCMAC is proposed and shown in Fig. 2, in which T denotes a time delay.

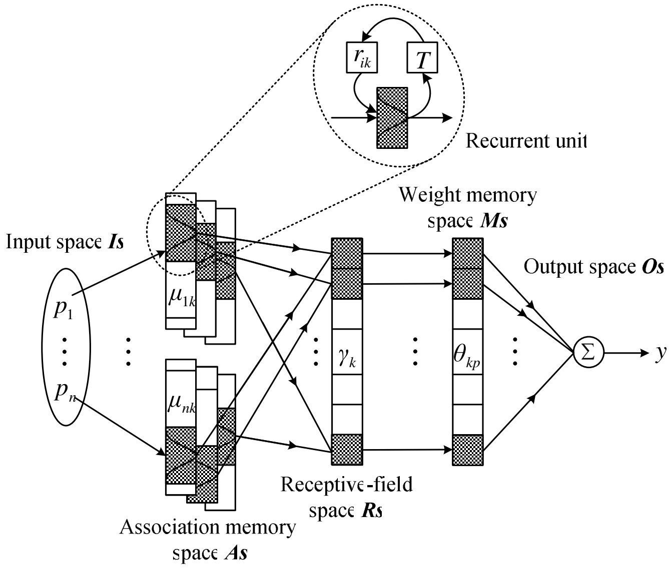

Fig. 2 RCMAC network architecture.

This RCMAC is composed of input space, association memory space with recurrent weights, receptive-field space, weight memory space and output space. The signal propagation and the basic function in each space are described as follows.

(1) *Input space Is*: For a given $\boldsymbol{p} = [p_1, p_2, \cdots, p_{n_a}]^T \in \Re^{n_a}$, where n_a is the number of input state variables of RCMAC, each input state variable p_i must be quantized into discrete regions (called *elements*) according to given control space. The number of elements, n_e, is termed as a resolution.

(2) *Association memory space As:* Several elements can be accumulated as a *block*, the number of blocks, n_b, is usually greater than or equal to two. *As* denotes an association memory space with n_c ($n_c = n_a \times n_b$) components. In this space, each block performs a receptive-field basis function, the Gaussian function is adopted here as the receptive-field basis function, which can be represented as

$$\mu_{ik} = exp\left[\frac{-(p_{rik} - m_{ik})^2}{\sigma_{ik}^2}\right], \text{ for } k = 1, 2, \cdots n_b \tag{9}$$

where μ_{ik} represents the output of the k-th block receptive-field basis function for the i-th input p_i with the mean m_{ik} and variance σ_{ik}. In addition, the input of this block can be represented as

$$p_{rik}(t) = p_i(t) + r_{ik}\,\boldsymbol{\mu}_{ik}(t-T) \tag{10}$$

where r_{ik} is the recurrent weight and $\mu_{ik}(t-T)$ denotes the value of μ_{ik} through delay time T. It is clear that the input of this block contains the memory term $\mu_{ik}(t-T)$, which stores the past information of the network and presents a dynamic mapping. Thus, the proposed RCMAC is more suitable for the dynamic function approximation. Figure 3 depicts the schematic diagram of a two-dimensional RCMAC with $n_e = 9$ and $\tau = 4$ (τ is the number of elements in a complete block); in which p_1 is divided into blocks B_{a1}, B_{b1} and B_{c1}, and p_2 is divided into blocks B_{a2}, B_{b2} and B_{c2}. By shifting each variable an element, different blocks can be obtained. For instance, blocks B_{d1}, B_{e1} and B_{f1} for p_1, and blocks B_{d2}, B_{e2} and B_{f2} for p_2 are possible shifted elements. Each block in this space has three adjustable parameters m_{ik}, σ_{ik} and r_{ik}.

(3) *Receptive-field space Rs*: Areas formed by blocks, referred to as $B_{a1}B_{a2}$, $B_{b1}B_{b2}$ and $B_{c1}B_{c2}$ are called receptive-fields. The number of receptive-fields, n_d, is equal to n_b in this study. The k-th multi-dimensional receptive-field function is defined as

$$\gamma_k(\boldsymbol{p}, \boldsymbol{m}_k, \boldsymbol{\sigma}_k, \boldsymbol{r}_k) = \prod_{i=1}^{n_a} \mu_{ik} = exp\left[\sum_{i=1}^{n_a} \frac{-(p_{rik} - m_{ik})^2}{\sigma_{ik}^2}\right]$$

for $k = 1, 2, \cdots n_d$ (11)

where $\boldsymbol{m}_k = [m_{1k}, m_{2k}, \cdots, m_{n_a k}]^T \in \Re^{n_a}$, $\boldsymbol{\sigma}_k = [\sigma_{1k}, \sigma_{2k}, \cdots, \sigma_{n_a k}]^T \in \Re^{n_a}$ and $\boldsymbol{r}_k = [r_{1k}, r_{2k}, \cdots, r_{n_a k}]^T \in \Re^{n_a}$. The multi-dimensional receptive-field functions can be expressed in a vector form as

$$\boldsymbol{\Gamma}(\boldsymbol{p}, \boldsymbol{m}, \boldsymbol{\sigma}, \boldsymbol{r}) = [\gamma_1, \cdots, \gamma_k, \cdots, \gamma_{n_d}]^T \tag{12}$$

Where $\boldsymbol{m} = [\boldsymbol{m}_1^T, \cdots, \boldsymbol{m}_k^T, \cdots, \boldsymbol{m}_{n_d}^T]^T \in \Re^{n_a n_d}$,

$\boldsymbol{\sigma} = [\boldsymbol{\sigma}_1^T, \cdots, \boldsymbol{\sigma}_k^T, \cdots, \boldsymbol{\sigma}_{n_d}^T]^T \in \Re^{n_a n_d}$ and $\boldsymbol{r} = [\boldsymbol{r}_1^T, \cdots, \boldsymbol{r}_k^T, \cdots, \boldsymbol{r}_{n_d}^T]^T \in \Re^{n_a n_d}$.

(4) *Weight memory space Ms:* Each location of *Rs* to a particular adjustable value in the weight memory space can be expressed as

$$\boldsymbol{\Theta} = [\boldsymbol{\theta}_1, \cdots, \boldsymbol{\theta}_p, \cdots, \boldsymbol{\theta}_{n_o}] = \begin{bmatrix} \theta_{11} & \cdots & \theta_{1p} & \cdots & \theta_{1n_o} \\ \vdots & \ddots & \vdots & \vdots & \vdots \\ \theta_{k1} & \cdots & \theta_{kp} & \cdots & \theta_{kn_o} \\ \vdots & \vdots & \vdots & \ddots & \vdots \\ \theta_{n_d 1} & \cdots & \theta_{n_d p} & \cdots & \theta_{n_d n_o} \end{bmatrix} \in \Re^{n_d \times n_o} \tag{13}$$

where $\boldsymbol{\theta}_p = [\theta_{1p}, \cdots \theta_{kp}, \cdots \theta_{n_d p}]^T \in \Re^{n_d}$, and θ_{kp} denotes the connecting weight value of the *p*-th output associated with the *k*-th receptive-field.

5) *Output space Os:* The output of RCMAC is the algebraic sum of the activated weights in the weight memory, and is expressed as

$$o_p = \boldsymbol{\theta}_p^T \boldsymbol{\Gamma} = \sum_{k=1}^{n_d} \theta_{kp} \gamma_k, \text{ for } p = 1, 2, \cdots n_o \tag{14}$$

The outputs of RCMAC can be expressed in a vector notation as

$$\boldsymbol{o} = [o_1, \cdots o_p, \cdots o_{n_o}]^T = \boldsymbol{\Theta}^T \boldsymbol{\Gamma} \tag{15}$$

In the two-dimensional case shown in Fig. 2, the output of RCMAC is the sum of the value in receptive-fields $B_{c1}B_{c2}$, $B_{f1}B_{f2}$, $B_{h1}B_{h2}$ and $B_{k1}B_{k2}$, when the input state is (7,7). The architecture of RCMAC used in this paper is designed to have the advantages of simple structure with dynamic characteristics. The role of the recurrent loops is to consider the past value of the receptive-field basis function in the association memory space. Thus, this RCMAC has dynamic characteristics.

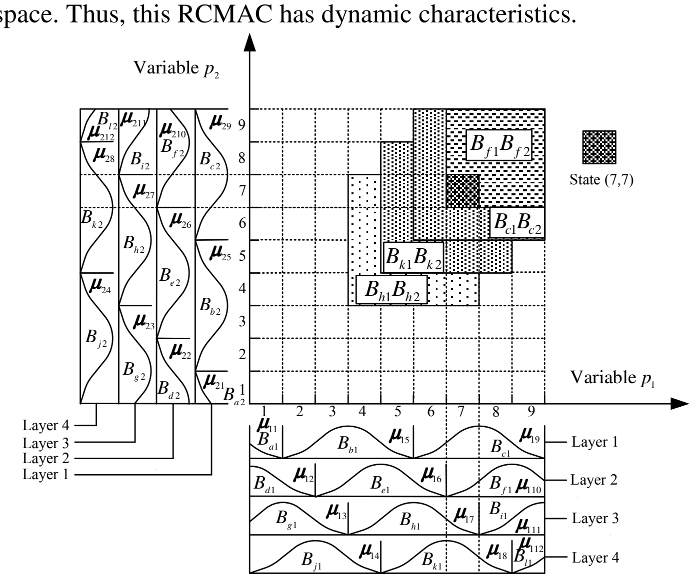

Fig. 3 Two-dimensional RCMAC with $n_e = 9$ and $\tau = 4$.

B. Adaptive laws and stability analysis

From Eqs. (3), (6) and (8), the system tracking error equation is obtained as follows:

$$\dot{\underline{\boldsymbol{\varepsilon}}} = \boldsymbol{\Xi}\, \underline{\boldsymbol{\varepsilon}} + \boldsymbol{\Psi}[\boldsymbol{u}_{id} - \hat{\boldsymbol{u}}_{RCMAC} - \boldsymbol{u}_H] \tag{16}$$

where

$$\boldsymbol{\Xi} = \begin{bmatrix} \mathbf{0} & \boldsymbol{I} & \mathbf{0} & \mathbf{0} & \cdots & \mathbf{0} & \mathbf{0} \\ \mathbf{0} & \mathbf{0} & \boldsymbol{I} & \mathbf{0} & \cdots & \mathbf{0} & \mathbf{0} \\ \vdots & \vdots & \vdots & \vdots & \ddots & \vdots & \vdots \\ \mathbf{0} & \mathbf{0} & \mathbf{0} & \mathbf{0} & \cdots & \mathbf{0} & \boldsymbol{I} \\ -\boldsymbol{L}_n & -\boldsymbol{L}_{n-1} & -\boldsymbol{L}_{n-2} & -\boldsymbol{L}_{n-3} & \cdots & -\boldsymbol{L}_2 & -\boldsymbol{L}_1 \end{bmatrix} \in \Re^{mn \times mn} \tag{17}$$

$$\boldsymbol{\Psi} = \begin{bmatrix} \mathbf{0} \\ \mathbf{0} \\ \vdots \\ \mathbf{0} \\ \boldsymbol{G}_n(\underline{\boldsymbol{x}}(t)) \end{bmatrix} \in \Re^{mn \times m} \tag{18}$$

By the universal approximation theory [27], theoretically there exists an optimal RCMAC $\boldsymbol{u}_{RCMAC}^*$ such that

$$\boldsymbol{u}_{id} = \boldsymbol{u}_{RCMAC}^*(\boldsymbol{p}, \boldsymbol{\Theta}^*, \boldsymbol{m}^*, \boldsymbol{\sigma}^*, \boldsymbol{r}^*) + \boldsymbol{\varpi} \equiv \boldsymbol{\Theta}^{*T} \boldsymbol{\Gamma}^*(\boldsymbol{m}^*, \boldsymbol{\sigma}^*, \boldsymbol{r}^*) + \boldsymbol{\varpi} \tag{19}$$

where $\boldsymbol{\varpi}$ denotes the approximation error vector; $\boldsymbol{\Theta}^*$ and $\boldsymbol{\Gamma}^*$ are the optimal parameter matrix and vector of $\boldsymbol{\Theta}$ and $\boldsymbol{\Gamma}$, respectively; and $\boldsymbol{m}^*$, $\boldsymbol{\sigma}^*$ and $\boldsymbol{r}^*$ are the optimal parameter vectors of $\boldsymbol{m}$, $\boldsymbol{\sigma}$ and $\boldsymbol{r}$, respectively. Since the optimal RCMAC can not be obtained, an RCMAC estimator is used to estimate the optimal RCMAC; this RCMAC estimator is defined as

$$\hat{\boldsymbol{u}}_{RCMAC}(\boldsymbol{p}, \hat{\boldsymbol{\Theta}}, \hat{\boldsymbol{m}}, \hat{\boldsymbol{\sigma}}, \hat{\boldsymbol{r}}) = \hat{\boldsymbol{\Theta}}^T \hat{\boldsymbol{\Gamma}}(\hat{\boldsymbol{m}}, \hat{\boldsymbol{\sigma}}, \hat{\boldsymbol{r}}) \tag{20}$$

where $\hat{\boldsymbol{\Theta}}$ and $\hat{\boldsymbol{\Gamma}}$ are the estimated matrix and vector of $\boldsymbol{\Theta}^*$ and $\boldsymbol{\Gamma}^*$, respectively; and $\hat{\boldsymbol{m}}, \hat{\boldsymbol{\sigma}}$ and $\hat{\boldsymbol{r}}$ are the estimated vectors of $\boldsymbol{m}^*$, $\boldsymbol{\sigma}^*$ and $\boldsymbol{r}^*$, respectively.

Subtracting Eqs. (19) and (20) into Eq. (16), yields

$$\dot{\underline{\boldsymbol{\varepsilon}}} = \boldsymbol{\Xi}\, \underline{\boldsymbol{\varepsilon}} + \boldsymbol{\Psi}[\boldsymbol{\Theta}^{*T} \boldsymbol{\Gamma}^* - \hat{\boldsymbol{\Theta}}^T \hat{\boldsymbol{\Gamma}} - \boldsymbol{u}_H + \boldsymbol{\varpi}] \tag{21}$$

Define $\tilde{\boldsymbol{\Theta}} = \boldsymbol{\Theta}^* - \hat{\boldsymbol{\Theta}}$ and $\tilde{\boldsymbol{\Gamma}} = \boldsymbol{\Gamma}^* - \hat{\boldsymbol{\Gamma}}$; then Eq. (21) becomes

$$\begin{aligned} \dot{\underline{\boldsymbol{\varepsilon}}} &= \boldsymbol{\Xi}\, \underline{\boldsymbol{\varepsilon}} + \boldsymbol{\Psi}[(\tilde{\boldsymbol{\Theta}} + \hat{\boldsymbol{\Theta}})^T (\tilde{\boldsymbol{\Gamma}} + \hat{\boldsymbol{\Gamma}}) - \hat{\boldsymbol{\Theta}}^T \hat{\boldsymbol{\Gamma}} - \boldsymbol{u}_H + \boldsymbol{\varpi}] \\ &= \boldsymbol{\Xi}\, \underline{\boldsymbol{\varepsilon}} + \boldsymbol{\Psi}[\hat{\boldsymbol{\Theta}}^T \tilde{\boldsymbol{\Gamma}} + \tilde{\boldsymbol{\Theta}}^T \hat{\boldsymbol{\Gamma}} + \tilde{\boldsymbol{\Theta}}^T \tilde{\boldsymbol{\Gamma}} - \boldsymbol{u}_H + \boldsymbol{\varpi}] \end{aligned} \tag{22}$$

Moreover, in order to achieve favorable estimation of dynamic function, the Taylor linearization technique is employed to transform the multi-dimensional receptive-field basis functions into a partially linear form. The expansion of $\tilde{\boldsymbol{\Gamma}}$ in Taylor series gets

$$\tilde{\boldsymbol{\Gamma}} = \begin{bmatrix} \tilde{\gamma}_1 \\ \tilde{\gamma}_2 \\ \vdots \\ \tilde{\gamma}_{n_d} \end{bmatrix} = \begin{bmatrix} \left(\dfrac{\partial \gamma_1}{\partial \boldsymbol{m}}\right)^T \\ \left(\dfrac{\partial \gamma_2}{\partial \boldsymbol{m}}\right)^T \\ \vdots \\ \left(\dfrac{\partial \gamma_{n_d}}{\partial \boldsymbol{m}}\right)^T \end{bmatrix} \Bigg|_{m=\hat{m}} (\boldsymbol{m}^* - \hat{\boldsymbol{m}}) + \begin{bmatrix} \left(\dfrac{\partial \gamma_1}{\partial \boldsymbol{\sigma}}\right)^T \\ \left(\dfrac{\partial \gamma_2}{\partial \boldsymbol{\sigma}}\right)^T \\ \vdots \\ \left(\dfrac{\partial \gamma_{n_d}}{\partial \boldsymbol{\sigma}}\right)^T \end{bmatrix} \Bigg|_{\sigma=\hat{\sigma}} (\boldsymbol{\sigma}^* - \hat{\boldsymbol{\sigma}})$$

$$+\begin{bmatrix} \left(\dfrac{\partial \gamma_1}{\partial \boldsymbol{r}}\right)^T \\ \left(\dfrac{\partial \gamma_2}{\partial \boldsymbol{r}}\right)^T \\ \vdots \\ \left(\dfrac{\partial \gamma_{n_d}}{\partial \boldsymbol{r}}\right)^T \end{bmatrix} |_{\boldsymbol{r}=\hat{\boldsymbol{r}}} \ (\boldsymbol{r}^* - \hat{\boldsymbol{r}}) + \boldsymbol{\Omega} \tag{23}$$

$$\tilde{\boldsymbol{\Gamma}} \equiv \boldsymbol{A}_m \tilde{\boldsymbol{m}} + \boldsymbol{B}_\sigma \tilde{\boldsymbol{\sigma}} + \boldsymbol{C}_r \tilde{\boldsymbol{r}} + \boldsymbol{\Omega} \tag{24}$$

where $\boldsymbol{A}_m = \left[\dfrac{\partial\gamma_1}{\partial \boldsymbol{m}}, \dfrac{\partial\gamma_2}{\partial \boldsymbol{m}}, \cdots, \dfrac{\partial\gamma_{n_d}}{\partial \boldsymbol{m}}\right]^T |_{\boldsymbol{m}=\hat{\boldsymbol{m}}} \in \Re^{n_d \times n_a n_d}$;

$\boldsymbol{B}_\sigma = \left[\dfrac{\partial\gamma_1}{\partial \boldsymbol{\sigma}}, \dfrac{\partial\gamma_2}{\partial \boldsymbol{\sigma}}, \cdots, \dfrac{\partial\gamma_{n_d}}{\partial \boldsymbol{\sigma}}\right]^T |_{\boldsymbol{\sigma}=\hat{\boldsymbol{\sigma}}} \in \Re^{n_d \times n_a n_d}$;

$\boldsymbol{C}_r = \left[\dfrac{\partial\gamma_1}{\partial \boldsymbol{r}}, \dfrac{\partial\gamma_2}{\partial \boldsymbol{r}}, \cdots, \dfrac{\partial\gamma_{n_d}}{\partial \boldsymbol{r}}\right]^T |_{\boldsymbol{r}=\hat{\boldsymbol{r}}} \in \Re^{n_d \times n_a n_d}$, $\tilde{\boldsymbol{m}} = \boldsymbol{m}^* - \hat{\boldsymbol{m}}$; $\tilde{\boldsymbol{\sigma}} = \boldsymbol{\sigma}^* - \hat{\boldsymbol{\sigma}}$; $\tilde{\boldsymbol{r}} = \boldsymbol{r}^* - \hat{\boldsymbol{r}}$ and $\boldsymbol{\Omega} \in \Re^{n_d}$ is a vector of higher-order terms. Moreover, $\dfrac{\partial \gamma_k}{\partial \boldsymbol{m}}$, $\dfrac{\partial \gamma_k}{\partial \boldsymbol{\sigma}}$ and $\dfrac{\partial \gamma_k}{\partial \boldsymbol{r}}$ are defined as

$$\left[\frac{\partial\gamma_k}{\partial \boldsymbol{m}}\right] = [\underbrace{0, \cdots, 0}_{(k-1)\times n_a}, \frac{\partial\gamma_k}{\partial m_{1k}}, \cdots, \frac{\partial\gamma_k}{\partial m_{n_a k}}, \underbrace{0, \cdots, 0}_{(n_d-k)\times n_a}] \tag{25}$$

$$\left[\frac{\partial\gamma_k}{\partial \boldsymbol{\sigma}}\right] = [\underbrace{0, \cdots, 0}_{(k-1)\times n_a}, \frac{\partial\gamma_k}{\partial \sigma_{1k}}, \cdots, \frac{\partial\gamma_k}{\partial \sigma_{n_a k}}, \underbrace{0, \cdots, 0}_{(n_d-k)\times n_a}] \tag{26}$$

$$\left[\frac{\partial\gamma_k}{\partial \boldsymbol{r}}\right] = [\underbrace{0, \cdots, 0}_{(k-1)\times n_a}, \frac{\partial\gamma_k}{\partial r_{1k}}, \cdots, \frac{\partial\gamma_k}{\partial r_{n_a k}}, \underbrace{0, \cdots, 0}_{(n_d-k)\times n_a}] \tag{27}$$

After substituting Eq. (24) into Eq. (22), the error equation can be rewritten as

$$\begin{aligned} \dot{\underline{\boldsymbol{\varepsilon}}} &= \boldsymbol{\Xi}\,\underline{\boldsymbol{\varepsilon}} + \boldsymbol{\Psi}[\hat{\boldsymbol{\Theta}}^T(\boldsymbol{A}_m\tilde{\boldsymbol{m}} + \boldsymbol{B}_\sigma\tilde{\boldsymbol{\sigma}} + \boldsymbol{C}_r\tilde{\boldsymbol{r}} + \boldsymbol{\Omega}) + \tilde{\boldsymbol{\Theta}}^T\hat{\boldsymbol{\Gamma}} + \tilde{\boldsymbol{\Theta}}^T\tilde{\boldsymbol{\Gamma}} - \boldsymbol{u}_H + \boldsymbol{\varpi}] \\ &= \boldsymbol{\Xi}\,\underline{\boldsymbol{\varepsilon}} + \boldsymbol{\Psi}[\hat{\boldsymbol{\Theta}}^T\boldsymbol{A}_m\tilde{\boldsymbol{m}} + \hat{\boldsymbol{\Theta}}^T\boldsymbol{B}_\sigma\tilde{\boldsymbol{\sigma}} + \hat{\boldsymbol{\Theta}}^T\boldsymbol{C}_r\tilde{\boldsymbol{r}} + \tilde{\boldsymbol{\Theta}}^T\hat{\boldsymbol{\Gamma}} + \boldsymbol{\omega} - \boldsymbol{u}_H] \end{aligned} \tag{28}$$

where the uncertain term $\boldsymbol{\omega} \equiv \hat{\boldsymbol{\Theta}}^T\boldsymbol{\Omega} + \tilde{\boldsymbol{\Theta}}^T\tilde{\boldsymbol{\Gamma}} + \boldsymbol{\varpi}$.

Then the following theorem can be stated and proved.

Theorem 1: Consider the MIMO uncertain nonlinear system represented by Eq. (1). The H^∞-tracking based adaptive hybrid control law is designed as Eq. (8); where $\hat{\boldsymbol{u}}_{RCMAC}$ is given from RCMAC output in Eq. (20) and the on-line parameter adaptive laws of RCMAC are designed as Eqs. (29)-(32)

$$\dot{\hat{\boldsymbol{\theta}}}_p = \alpha_1\,\hat{\boldsymbol{\Gamma}}\,\boldsymbol{\psi}_p^T\boldsymbol{P}\,\underline{\boldsymbol{\varepsilon}} \tag{29}$$

$$\dot{\hat{\boldsymbol{m}}} = \alpha_2\,\boldsymbol{A}_m^T\,\hat{\boldsymbol{\Theta}}\,\boldsymbol{\Psi}^T\boldsymbol{P}\underline{\boldsymbol{\varepsilon}} \tag{30}$$

$$\dot{\hat{\boldsymbol{\sigma}}} = \alpha_3\,\boldsymbol{B}_\sigma^T\hat{\boldsymbol{\Theta}}\,\boldsymbol{\Psi}^T\boldsymbol{P}\underline{\boldsymbol{\varepsilon}} \tag{31}$$

$$\dot{\hat{\boldsymbol{r}}} = \alpha_4\,\boldsymbol{C}_r^T\hat{\boldsymbol{\Theta}}\,\boldsymbol{\Psi}^T\boldsymbol{P}\underline{\boldsymbol{\varepsilon}} \tag{32}$$

where $\dot{\hat{\boldsymbol{\theta}}}_p$ is the p-th column of matrix $\dot{\hat{\boldsymbol{\Theta}}}$, $\boldsymbol{\psi}_p$ is the p-th column of matrix $\boldsymbol{\Psi}$, and α_1, α_2, α_3 and α_4 are the learning-rates with positive constants. The compensation controller is designed as

$$\boldsymbol{u}_H = \boldsymbol{R}^{-1}\boldsymbol{\Psi}^T\boldsymbol{P}\underline{\boldsymbol{\varepsilon}} \tag{33}$$

where there exist a symmetric positive definite matrix $\boldsymbol{P}$ and a positive definite matrix $\boldsymbol{Z}$ satisfying the following Riccati-like equation

$$\boldsymbol{\Xi}^T\boldsymbol{P} + \boldsymbol{P}\boldsymbol{\Xi} - 2\boldsymbol{P}\boldsymbol{\Psi}(\boldsymbol{R}^{-1} - \frac{1}{2\rho^2}\boldsymbol{I})\boldsymbol{\Psi}^T\boldsymbol{P} = -\boldsymbol{Z} \tag{34}$$

in which $\boldsymbol{R}^{-1} \geq 2\rho^2\boldsymbol{I}$ is a designed diagonal matrix and ρ is an attenuation level for the uncertainty. Then the overall control system guarantees the following H^∞-tracking performance

$$\int_0^t \underline{\boldsymbol{\varepsilon}}^T\underline{\boldsymbol{\varepsilon}}\,d\boldsymbol{\tau} \leq \frac{2}{\boldsymbol{\lambda}_{min}(\boldsymbol{Z})}V(0) + \frac{\rho^2}{\boldsymbol{\lambda}_{min}(\boldsymbol{Z})}\int_0^t \boldsymbol{\omega}^T\boldsymbol{\omega}\,d\boldsymbol{\tau} \tag{35}$$

where $\boldsymbol{\lambda}_{min}(\boldsymbol{Z})$ denotes the minimum eigenvalue of $\boldsymbol{Z}$.

Proof: Consider the following Lyapunov function

$$\begin{aligned} V(\underline{\boldsymbol{\varepsilon}}, \tilde{\boldsymbol{\Theta}}, \tilde{\boldsymbol{m}}, \tilde{\boldsymbol{\sigma}}, \tilde{\boldsymbol{r}}) &= \frac{1}{2}\underline{\boldsymbol{\varepsilon}}^T\boldsymbol{P}\underline{\boldsymbol{\varepsilon}} + \frac{1}{2\alpha_1}tr\,(\tilde{\boldsymbol{\Theta}}^T\,\tilde{\boldsymbol{\Theta}}) + \frac{1}{2\alpha_2}\tilde{\boldsymbol{m}}^T\tilde{\boldsymbol{m}} \\ &+ \frac{1}{2\alpha_3}\tilde{\boldsymbol{\sigma}}^T\tilde{\boldsymbol{\sigma}} + \frac{1}{2\alpha_4}\tilde{\boldsymbol{r}}^T\tilde{\boldsymbol{r}} \end{aligned} \tag{36}$$

Taking the derivative of time for the Lyapunov function, yields

$$\begin{aligned} \dot{V}(\underline{\boldsymbol{\varepsilon}}, \tilde{\boldsymbol{\Theta}}, \tilde{\boldsymbol{m}}, \tilde{\boldsymbol{\sigma}}, \tilde{\boldsymbol{r}}) &= \frac{1}{2}[\dot{\underline{\boldsymbol{\varepsilon}}}^T\boldsymbol{P}\underline{\boldsymbol{e}} + \underline{\boldsymbol{\varepsilon}}^T\boldsymbol{P}\dot{\underline{\boldsymbol{\varepsilon}}}] + \frac{1}{\alpha_1}tr\,(\tilde{\boldsymbol{\Theta}}^T\,\dot{\tilde{\boldsymbol{\Theta}}}) \\ &+ \frac{1}{\alpha_2}\tilde{\boldsymbol{m}}^T\dot{\tilde{\boldsymbol{m}}} + \frac{1}{\alpha_3}\tilde{\boldsymbol{\sigma}}^T\dot{\tilde{\boldsymbol{\sigma}}} + \frac{1}{\alpha_4}\tilde{\boldsymbol{r}}^T\dot{\tilde{\boldsymbol{r}}} \end{aligned} \tag{37}$$

Substituting Eq. (28) into Eq. (37) and from Eq. (34), yields

$$\begin{aligned} \dot{V}(\underline{\boldsymbol{\varepsilon}}, \tilde{\boldsymbol{\Theta}}, \tilde{\boldsymbol{m}}, \tilde{\boldsymbol{\sigma}}, \tilde{\boldsymbol{r}}) &= \frac{1}{2}\underline{\boldsymbol{\varepsilon}}^T[\boldsymbol{\Xi}^T\boldsymbol{P} + \boldsymbol{P}\boldsymbol{\Xi}]\,\underline{\boldsymbol{\varepsilon}} + [\tilde{\boldsymbol{m}}^T\boldsymbol{A}_m^T\,\hat{\boldsymbol{\Theta}} + \tilde{\boldsymbol{\sigma}}^T\boldsymbol{B}_\sigma^T\,\hat{\boldsymbol{\Theta}} \\ &+ \tilde{\boldsymbol{r}}^T\boldsymbol{C}_r^T\,\hat{\boldsymbol{\Theta}} + \hat{\boldsymbol{\Gamma}}^T\tilde{\boldsymbol{\Theta}} + \boldsymbol{\omega}^T - \boldsymbol{u}_H^T]\boldsymbol{\Psi}^T\boldsymbol{P}\underline{\boldsymbol{\varepsilon}} \\ &+ \frac{1}{\alpha_1}tr\,(\tilde{\boldsymbol{\Theta}}^T\,\dot{\tilde{\boldsymbol{\Theta}}}) + \frac{1}{\alpha_1}tr\,(\tilde{\boldsymbol{\Theta}}^T\,\dot{\tilde{\boldsymbol{\Theta}}}) + \frac{1}{\alpha_2}\tilde{\boldsymbol{m}}^T\dot{\tilde{\boldsymbol{m}}} \\ &+ \frac{1}{\alpha_3}\tilde{\boldsymbol{\sigma}}^T\dot{\tilde{\boldsymbol{\sigma}}} + \frac{1}{\alpha_4}\tilde{\boldsymbol{r}}^T\dot{\tilde{\boldsymbol{r}}} \\ &= -\frac{1}{2}\underline{\boldsymbol{\varepsilon}}^T\boldsymbol{Z}\underline{\boldsymbol{\varepsilon}} + \underline{\boldsymbol{\varepsilon}}^T\boldsymbol{P}\boldsymbol{\Psi}\,[\boldsymbol{R}^{-1}\boldsymbol{\Psi}^T\boldsymbol{P}\underline{\boldsymbol{\varepsilon}} - \boldsymbol{u}_H] \\ &- \frac{1}{2\boldsymbol{\rho}^2}\underline{\boldsymbol{\varepsilon}}^T\boldsymbol{P}\boldsymbol{\Psi}\boldsymbol{\Psi}^T\boldsymbol{P}\underline{\boldsymbol{\varepsilon}} + \hat{\boldsymbol{\Gamma}}^T\tilde{\boldsymbol{\Theta}}\boldsymbol{\Psi}^T\boldsymbol{P}\underline{\boldsymbol{\varepsilon}} \\ &+ \frac{1}{\alpha_1}tr(\tilde{\boldsymbol{\Theta}}^T\,\dot{\tilde{\boldsymbol{\Theta}}}) + \tilde{\boldsymbol{m}}^T\boldsymbol{A}_m^T\hat{\boldsymbol{\Theta}}\boldsymbol{\Psi}^T\boldsymbol{P}\underline{\boldsymbol{\varepsilon}} + \frac{1}{\alpha_2}\tilde{\boldsymbol{m}}^T\dot{\tilde{\boldsymbol{m}}} \\ &+ \tilde{\boldsymbol{\sigma}}^T\boldsymbol{B}_\sigma^T\hat{\boldsymbol{\Theta}}\boldsymbol{\Psi}^T\boldsymbol{P}\underline{\boldsymbol{\varepsilon}} + \frac{1}{\alpha_3}\tilde{\boldsymbol{\sigma}}^T\dot{\tilde{\boldsymbol{\sigma}}} + \tilde{\boldsymbol{r}}^T\boldsymbol{C}_r^T\hat{\boldsymbol{\Theta}}\boldsymbol{\Psi}^T\boldsymbol{P}\underline{\boldsymbol{\varepsilon}} \\ &+ \frac{1}{\alpha_4}\tilde{\boldsymbol{r}}^T\dot{\tilde{\boldsymbol{r}}} + \boldsymbol{\omega}^T\boldsymbol{\Psi}^T\boldsymbol{P}\underline{\boldsymbol{\varepsilon}} \end{aligned} \tag{38}$$

Noting in Eq. (38), that

$$\frac{1}{\alpha_1}tr\,(\tilde{\boldsymbol{\Theta}}^T\,\dot{\tilde{\boldsymbol{\Theta}}}) = \frac{1}{\alpha_1}\sum_{p=1}^{n_o}\tilde{\boldsymbol{\theta}}_p^T\dot{\tilde{\boldsymbol{\theta}}}_p \tag{39}$$

$$\hat{\boldsymbol{\Gamma}}^T\tilde{\boldsymbol{\Theta}}\boldsymbol{\Psi}^T\boldsymbol{P}\underline{\boldsymbol{\varepsilon}} = \sum_{p=1}^{n_o}\hat{\boldsymbol{\Gamma}}^T\tilde{\boldsymbol{\theta}}_p\boldsymbol{\psi}_p^T\boldsymbol{P}\underline{\boldsymbol{\varepsilon}} \tag{40}$$

From the definition of $\boldsymbol{u}_H$ in Eq. (33), it is obtained that

$$\dot{V}(\underline{\varepsilon},\tilde{\boldsymbol{\Theta}},\tilde{\boldsymbol{m}},\tilde{\boldsymbol{\sigma}},\tilde{\boldsymbol{r}}) = -\frac{1}{2}\underline{\varepsilon}^T\boldsymbol{Z}\underline{\varepsilon} - \frac{1}{2\rho^2}\underline{\varepsilon}^T\boldsymbol{P\Psi\Psi}^T\boldsymbol{P}\underline{\varepsilon}$$
$$+\sum_{p=1}^{n_o}\tilde{\boldsymbol{\theta}}_p^T[\hat{\boldsymbol{\Gamma}}\,\boldsymbol{\psi}_p^T\boldsymbol{P}\underline{\varepsilon} + \frac{1}{\alpha_1}\dot{\tilde{\boldsymbol{\theta}}}_p]$$
$$+\tilde{\boldsymbol{m}}^T[\boldsymbol{A}_m^T\hat{\boldsymbol{\Theta}}\boldsymbol{\Psi}^T\boldsymbol{P}\underline{\varepsilon} + \frac{1}{\alpha_2}\dot{\tilde{\boldsymbol{m}}}]$$
$$+\tilde{\boldsymbol{\sigma}}^T[\boldsymbol{B}_\sigma^T\hat{\boldsymbol{\Theta}}\boldsymbol{\Psi}^T\boldsymbol{P}\underline{\varepsilon} + \frac{1}{\alpha_3}\dot{\tilde{\boldsymbol{\sigma}}}]$$
$$+\tilde{\boldsymbol{r}}^T[\boldsymbol{C}_r^T\hat{\boldsymbol{\Theta}}\boldsymbol{\Psi}^T\boldsymbol{P}\underline{\varepsilon} + \frac{1}{\alpha_4}\dot{\tilde{\boldsymbol{r}}}] + \underline{\varepsilon}^T\boldsymbol{P\Psi\omega} \tag{41}$$

where $\dot{\tilde{\boldsymbol{\theta}}}_p$ is the p-th column of matrix $\dot{\tilde{\boldsymbol{\Theta}}}$. Using the adaptive laws in Eqs. (29)-(32), Eq. (41) can be rewritten as

$$\dot{V}(\underline{\varepsilon},\tilde{\boldsymbol{\Theta}},\tilde{\boldsymbol{m}},\tilde{\boldsymbol{\sigma}},\tilde{\boldsymbol{r}}) = -\frac{1}{2}\underline{\varepsilon}^T\boldsymbol{Z}\underline{\varepsilon} - \frac{1}{2\rho^2}\underline{\varepsilon}^T\boldsymbol{P\Psi\Psi}^T\boldsymbol{P}\underline{\varepsilon} + \underline{\varepsilon}^T\boldsymbol{P\Psi}\,\boldsymbol{\omega}$$
$$= -\frac{1}{2}\underline{\varepsilon}^T\boldsymbol{Z}\underline{\varepsilon} + \frac{\rho^2}{2}\boldsymbol{\omega}^T\boldsymbol{\omega} - \frac{1}{2}[\frac{1}{\rho^2}\underline{\varepsilon}^T\boldsymbol{P\Psi\Psi}^T\boldsymbol{P}\underline{\varepsilon}$$
$$-2\frac{\underline{\varepsilon}^T\boldsymbol{P\Psi}}{\rho}\rho\,\boldsymbol{\omega} + \boldsymbol{\rho}^2\boldsymbol{\omega}^T\boldsymbol{\omega}]$$
$$= -\frac{1}{2}\underline{\varepsilon}^T\boldsymbol{Z}\underline{\varepsilon} + \frac{\rho^2}{2}\boldsymbol{\omega}^T\boldsymbol{\omega}$$
$$-\frac{1}{2}[\frac{1}{\rho}\boldsymbol{\Psi}^T\boldsymbol{P}\underline{\varepsilon} - \rho\,\boldsymbol{\omega}]^T[\frac{1}{\rho}\boldsymbol{\Psi}^T\boldsymbol{P}\underline{\varepsilon} - \rho\,\boldsymbol{\omega}]$$
$$\le -\frac{1}{2}\underline{\varepsilon}^T\boldsymbol{Z}\underline{\varepsilon} + \frac{\rho^2}{2}\boldsymbol{\omega}^T\boldsymbol{\omega} \tag{42}$$

Now integrating the above inequality, it is obtained that

$$V(t) - V(0) \le -\frac{1}{2}\int_0^t \underline{\varepsilon}^T\boldsymbol{Z}\underline{\varepsilon}\,d\boldsymbol{\tau} + \frac{\rho^2}{2}\int_0^t \boldsymbol{\omega}^T\boldsymbol{\omega}\,d\boldsymbol{\tau} \tag{43}$$

Since $V(t) \ge 0$, the following H^∞ criterion can be obtained

$$\frac{1}{2}\int_0^t \underline{\varepsilon}^T\boldsymbol{Z}\underline{\varepsilon}\,d\boldsymbol{\tau} \le V(0) + \frac{\rho^2}{2}\int_0^t \boldsymbol{\omega}^T\boldsymbol{\omega}\,d\boldsymbol{\tau} \tag{44}$$

Because $\boldsymbol{Z}$ is a positive definite matrix and from the fact that $\lambda_{min}(\boldsymbol{Z})\underline{\varepsilon}^T\underline{\varepsilon} \le \underline{\varepsilon}^T\boldsymbol{Z}\underline{\varepsilon}$, it implies

$$\frac{\boldsymbol{\lambda}_{min}(\boldsymbol{Z})}{2}\int_0^t \underline{\varepsilon}^T\underline{\varepsilon}\,d\boldsymbol{\tau} \le V(0) + \frac{\rho^2}{2}\int_0^t \boldsymbol{\omega}^T\boldsymbol{\omega}\,d\boldsymbol{\tau} \tag{45}$$

Thus the inequality (35) is proved.

IV. SIMULATION STUDIES

To verify the effectiveness of the proposed approach, the developed H^∞-tracking based adaptive control scheme is applied to control two MIMO uncertain nonlinear systems, a one-link rigid robotic manipulator and a mass-spring-damper mechanical system.

Example 1. One-link rigid robotic manipulator

The dynamic equation of one-link rigid robotic manipulator is given by

$$ml^2\ddot{q} + b\dot{q} + ml\,g_v\cos(q) = u \tag{46}$$

where the link is of length l and mass m, and q is the angular position with initial values $q(0) = 0.1$ and $\dot{q}(0) = 0$. The above dynamical equation can be written as the following state equation:

$$\begin{bmatrix}\dot{x}_1\\ \dot{x}_2\end{bmatrix} = \begin{bmatrix}0 & 1\\ 0 & 0\end{bmatrix}\begin{bmatrix}x_1\\ x_2\end{bmatrix} + \begin{bmatrix}0\\ 1\end{bmatrix}(f + gu + d) \tag{47}$$

where $x_1 = q$, $x_2 = \dot{q}$, $f = \frac{-b}{ml^2}x_2 - \frac{g_v}{l}\cos(x_1)$, $g = \frac{1}{ml^2}$, the parameters in (47) are chosen as $m = l = b = g_v = 1$, and d is a square wave external disturbance with amplitude ± 0.1 and period 2π. The reference model is given as

$$\begin{bmatrix}\dot{x}_{d1}\\ \dot{x}_{d2}\end{bmatrix} = \begin{bmatrix}0 & 1\\ -16 & -8\end{bmatrix}\begin{bmatrix}x_{d1}\\ x_{d2}\end{bmatrix} + \begin{bmatrix}0\\ 1\end{bmatrix}u_d(t) \tag{48}$$

where $[x_{d1}(0), x_{d2}(0)]^T = [0, 0]$ and $u_d(t)$ is a periodic rectangular signal. For the H^∞-tracking based adaptive control scheme, the feedback gain is designed as $\underline{\boldsymbol{L}} = [9, 6]^T$. For a choice of $\boldsymbol{Z} = \begin{bmatrix}90 & 9\\ 9 & 2\end{bmatrix}$ and solving the Riccati-like equation that shown in Eq. (34) with $\boldsymbol{R} = 2\rho^2\boldsymbol{I}$, it can be obtained that

$$P = \begin{bmatrix}30 & 5\\ 5 & 1\end{bmatrix} \tag{49}$$

The designed RCMAC is characterized as:

- number of elements for each state variable: $n_e = 9$ (elements)
- generalization: $\tau = 4$ (elements/ block)
- number of blocks for each state variable: $n_b = 3$ (blocks/layer) $\times 4$ (layer) $= 12$ (blocks)
- number of receptive-fields: $n_d = 3$ (receptive-fields/layer) $\times 4$ (layer) $= 12$ (receptive-fields)
- receptive-field basis functions: $\mu_{ik} = exp[-(p_{rik} - m_{ik})^2 / \sigma_{ik}^2]$ for $i = 1, 2$ and $k = 1, 2, \cdots, 12$

The initial means of the Gaussian functions are divided equally and are set as $m_{i1} = -0.40$, $m_{i2} = -0.32$, $m_{i3} = -0.28$, $m_{i4} = -0.20$, $m_{i5} = -0.12$, $m_{i6} = -0.04$, $m_{i7} = 0.04$, $m_{i8} = 0.12$, $m_{i9} = 0.20$, $m_{i10} = 0.28$, $m_{i11} = 0.32$, $m_{i12} = 0.40$ and the initial variances are set as $\sigma_{ik} = 0.2$ for $i = 1, 2$ and $k = 1, 2, \cdots, 12$. These parameters are chosen to cover the input signal space and through the basic principle presented in (Wang, 1994). The learning-rates of RCMAC are chosen as $\alpha_1 = 6.25$, $\alpha_2 = 0.75$, $\alpha_3 = 0.75$ and $\alpha_4 = 0.01$. To investigate the effectiveness of compensation controller, different ρ's are used for simulations. Firstly, the simulation results for one-link rigid robotic manipulator with $\rho = 1$ are shown in Fig. 4. Figures. 4(a) and 4(b) represent the trajectory of position and velocity, respectively. The associated control effort $u(t)$ is depicted in Fig. 4(c), and the tracking error is shown in Fig. 4(d). The simulation results show that the tracking response in transient state is not good enough due to large attenuation level ρ. The simulation results with $\rho = 0.1$ are shown in Fig. 5, which shows the favorable control performance with small tracking error. Thus, the proposed H^{∞}-tracking based adaptive control system can achieve better performance as the attenuation level ρ is specified smaller.

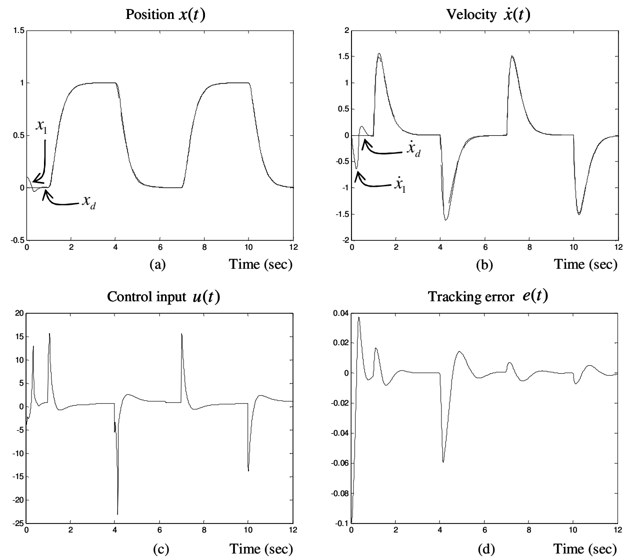

Fig. 4 Time responses for one-link rigid robotic manipulator with $\rho = 1$.

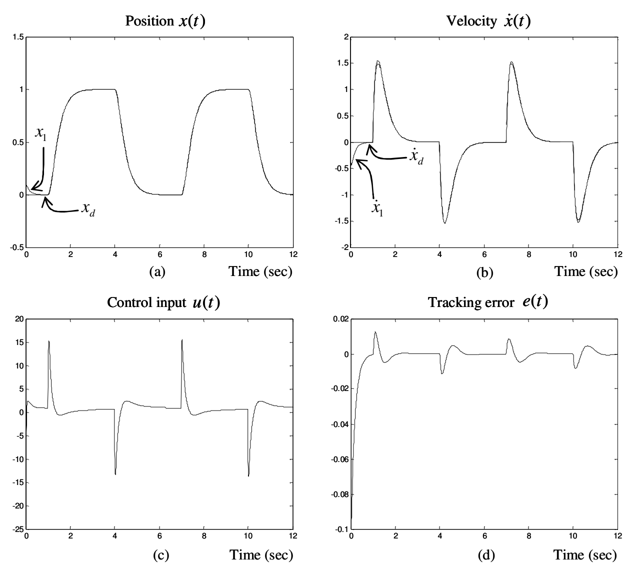

Fig. 5 Time responses for one-link rigid robotic manipulator with $\rho = 0.1$

Example 2. Mass-spring-damper mechanical system

A mass-spring-damper mechanical system is shown in Fig. 6.

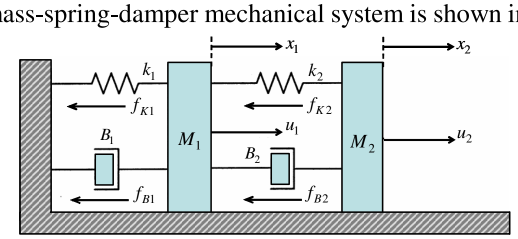

Fig. 6 Mass-spring-damper system.

The dynamic equations of this mechanical system are expressed as [4]

$$M_1\ddot{x}_1(t) = -f_{K1}(\underline{\boldsymbol{x}}) - f_{B1}(\underline{\boldsymbol{x}}) + f_{K2}(\underline{\boldsymbol{x}}) + f_{B2}(\underline{\boldsymbol{x}}) + u_1(t) + \Delta u_{12}(t) + \delta_1(t) \tag{50}$$

$$M_2\ddot{x}_2(t) = -f_{K2}(\underline{\boldsymbol{x}}) - f_{B2}(\underline{\boldsymbol{x}}) + u_2 + \Delta u_{21} + \delta_2(t) \tag{51}$$

where M_1 and M_2 are the masses of the system, and $\underline{\boldsymbol{x}}(t) = [x_1(t), x_2(t), \dot{x}_1(t), \dot{x}_2(t)]^T$ are the positions and velocities of the mechanical system. The spring forces $f_{K1}(\underline{\boldsymbol{x}}) = k_{10}x_1 + \Delta k_1 x_1^3$, $f_{K2}(\underline{\boldsymbol{x}}) = k_{20}(x_2 - x_1) + \Delta k_2(x_2 - x_1)^3$ and the friction forces $f_{B1}(\underline{\boldsymbol{x}}) = b_{10}\dot{x}_1 + \Delta b_1 \dot{x}_1^2$, $f_{B2}(\underline{\boldsymbol{x}}) = b_{20}(\dot{x}_2 - \dot{x}_1) + \Delta b_2(\dot{x}_2 - \dot{x}_1)^2$. The parameters of system are given as $M_1 = 1$, $M_2 = 0.8$, $k_{10} = 3$, $k_{20} = 4$, $b_{10} = 2$, $b_{20} = 2.2$, $\Delta k_1 = 0.5$, $\Delta k_2 = 0.5$, $\Delta b_1 = 0.5$, $\Delta b_2 = 0.5$, $\Delta u_{12} = 0.2u_2$, $\Delta u_{21} = 0.25u_1$, $\boldsymbol{\delta}_1(t) = 2exp(-0.2t)$ and $\boldsymbol{\delta}_2(t) = -2exp(-0.1t)$.

Consequently, the dynamic equation of the mass-spring-damper mechanical system can be rewritten as

$$\ddot{\boldsymbol{x}}(t) = \boldsymbol{f}(\underline{\boldsymbol{x}}) + \boldsymbol{G}(\underline{\boldsymbol{x}})\boldsymbol{u}(t) + \boldsymbol{d}(t) \tag{52}$$

where

$$\boldsymbol{f}(\underline{\boldsymbol{x}}) = \begin{bmatrix} \dfrac{-f_{K1}(\underline{\boldsymbol{x}}) - f_{B1}(\underline{\boldsymbol{x}}) + f_{K2}(\underline{\boldsymbol{x}}) + f_{B2}(\underline{\boldsymbol{x}})}{M_1} \\ \dfrac{-f_{K2}(\underline{\boldsymbol{x}}) - f_{B2}(\underline{\boldsymbol{x}})}{M_2} \end{bmatrix},$$

$\boldsymbol{G}(\underline{\boldsymbol{x}}) = \begin{bmatrix} \dfrac{1}{M_1} & \dfrac{0.2}{M_1} \\ \dfrac{0.25}{M_2} & \dfrac{1}{M_2} \end{bmatrix}$ and $\boldsymbol{u}(t) \triangleq [u_1(t), u_2(t)]^T$ denotes the control input and $\boldsymbol{d}(t) \triangleq [\dfrac{\boldsymbol{\delta}_1(t)}{M_1}, \dfrac{\boldsymbol{\delta}_2(t)}{M_2}]^T$ denotes the external disturbance. The desired trajectories come from the reference model outputs, the reference model is chosen as $\ddot{x}_{dm}(t) = -16x_{dm}(t) - 8\dot{x}_{dm}(t) + 16r_m$, $m = 1, 2$. The initial conditions of the mechanical system and the reference model are given as $x_2(0) = 1$, $\dot{x}_2(0) = 0$, $x_{d1}(0) = 0$, $\dot{x}_{d1}(0) = 0$, $x_{d2}(0) = 0$ and $\dot{x}_{d2}(0) = 0$. The reference inputs are $r_1 = \dfrac{\boldsymbol{\pi}}{3}(0.9sin(\dfrac{t}{2}) + 0.1sin(2t))$ and $r_2 = \boldsymbol{\pi}(0.4sin(t) + 0.1sin(3t))$.

For the proposed H^{∞}-tracking based adaptive control scheme, the feedback gain matrix is designed as $\underline{\boldsymbol{L}} = [\boldsymbol{L}_2, \boldsymbol{L}_1]^T$, in which $\boldsymbol{L}_1 = diag(20, 20)$ and $\boldsymbol{L}_2 = diag(100, 100)$. For a choice of $\boldsymbol{Z} = diag(100, 100, 10, 10)$ and to solve the Riccati-like equation shown in Eq. (34) with $\boldsymbol{R} = 2\rho^2\boldsymbol{I}$, it can be obtained that

$$\boldsymbol{P}=\begin{bmatrix}37.5 & 0 & 0.5 & 0\\ 0 & 37.5 & 0 & 0.5\\ 0.5 & 0 & 0.275 & 0\\ 0 & 0.5 & 0 & 0.275\end{bmatrix} \quad (53)$$

The designed RCMAC is characterized as:

- number of elements for each state variable: $n_e = 9$ (elements)
- generalization: $\tau = 4$ (elements/ block)
- number of blocks for each state variable: $n_b = 3$ (blocks/layer)$\times 4$ (layer) $= 12$ (blocks)
- number of receptive-fields: $n_d = 3$ (receptive-fields/layer) $\times 4$ (layer) $= 12$ (receptive-fields)
- receptive-field basis functions: $\boldsymbol{\mu}_{ik} = exp[-(p_{rik} - m_{ik})^2 / \sigma_{ik}^2]$ for $i = 1, 2, 3, 4$ and $k = 1, 2, \cdots, 12$.

The initial means of the Gaussian functions are divided equally and are set as $m_{i1} = -2.2$, $m_{i2} = -1.8$, $m_{i3} = -1.4$, $m_{i4} = -1$, $m_{i5} = -0.6$, $m_{i6} = -0.2$, $m_{i7} = 0.2$, $m_{i8} = 0.6$, $m_{i9} = 1$, $m_{i10} = 1.4$, $m_{i11} = 1.8$, $m_{i12} = 2.2$ and the initial variances are set as $\sigma_{ik} = 0.8$ for $i = 1, 2, 3, 4$ and $k = 1, 2, \cdots, 12$. The learning-rates of RCMAC are chosen as $\alpha_1 = 6$, $\alpha_2 = 0.06$, $\alpha_3 = 0.06$ and $\alpha_4 = 0.04$. To investigate the effectiveness of compensation controller, different ρ 's are used for simulations. Firstly, the simulation results for mass-spring-damper mechanical system with $\rho = 1$ is shown in Fig. 7. Figures. 7(a) and 7(b) represent the trajectories of positions $x_1(t)$ and $x_2(t)$, respectively; the trajectories of velocities $\dot{x}_1(t)$ and $\dot{x}_2(t)$ are plotted in Figs. 7(c) and 7(d), respectively. The associated control efforts $u_1(t)$ and $u_2(t)$ are depicted in Figs. 7(e) and 7(f), respectively. The simulation results show that the tracking responses in transient state are not good enough. This is because the attenuation level ρ is chosen too large so that the residual approximation error can not be eliminated appropriately, thus the robust tracking performance can not be yielded. Secondly, the simulation results with $\rho = 0.1$ are shown in Fig. 8. From the simulation results, it can be seen that favorable tracking performance can be obtained without precisely knowledge of system dynamic function; moreover, it can achieve better tracking performance as the attenuation level ρ is specified smaller.

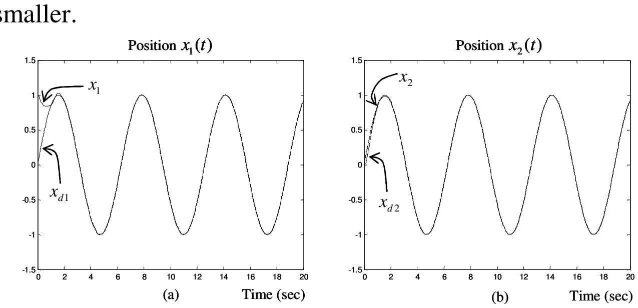

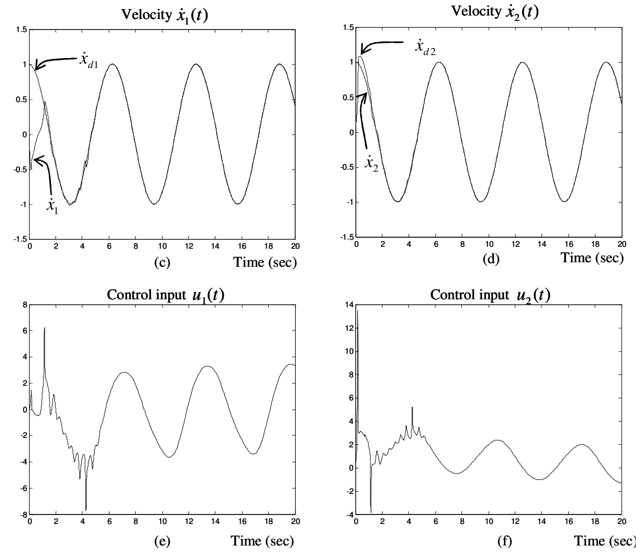

Fig. 7 Time responses for mass-spring-damper system with $\rho = 1$

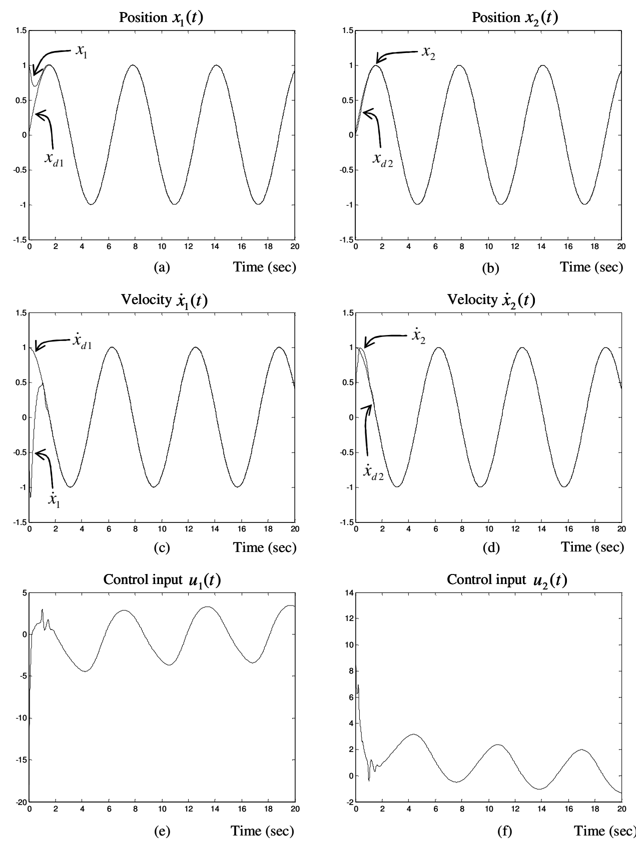

Fig. 8 Time responses for mass-spring-damper system with $\rho = 0.1$

V. Conclusions

A H^∞-tracking based adaptive control scheme has been proposed for uncertain nonlinear systems. The proposed control scheme is comprised of a recurrent cerebellar model articulation controller (RCMAC) and a compensation controller. RCMAC is utilized to approximate an ideal controller and the compensation controller is utilized to attenuate the residual approximation error with a specified H^∞-tracking performance.

The effectiveness of the proposed control system is verified by controlling two nonlinear systems, a one-link rigid robotic manipulator and a mass-spring-damper mechanical system. The simulation results confirm that the proposed H^{∞}-tracking based adaptive control scheme can guarantee a favorable tracking performance by specifying a desired robust attenuation level.

REFERENCES

[1] Albus, J. S. (1975). A new approach to manipulator control: The cerebellar model articulation controller (CMAC). *Journal of Dynamic System Measurement and Control*, *97*(3), 220-227.

[2] Chang, Y. C. (2001). A robust tracking control for chaotic Chua's circuits via fuzzy approach. *IEEE Transactions on Circuits and Systems—Part I: Fundamental Theory and Applications*, *48*(7), 889-895.

[3] Chang, Y. C. (2005). Intelligent robust control for uncertain nonlinear time-varying systems and its application to robotic system. *IEEE Transactions on Systems, Man, and Cybernetics, Part B: Cybernetics*, *35*(6), 1108-1119.

[4] Chang, Y. C., & Yen, H. M. (2005). Adaptive output feedback tracking control for a class of uncertain nonlinear systems using neural networks. *IEEE Transactions on Systems, Man, and Cybernetics, Part B: Cybernetics*, *35*(6), 1311-1316.

[5] Chen, B. S., Lee, C. H., & Chang, Y. C. (1996). H^{∞} tracking design of uncertain nonlinear SISO systems: adaptive fuzzy approach. *IEEE Transactions on Fuzzy Systems*, *4*(1), 32-43.

[6] Ge, S. S., & Wang, J. (2002). Robust adaptive neural control for a class of perturbed strict feedback nonlinear systems. *IEEE Transactions on Neural Networks*, *13*(6), 1409-1419.

[7] Gonzalez-Serrano, F. J., Figueiras-Vidal, A. R., & Artes-Rodriguez, A. (1998). Generalizing CMAC architecture and training. *IEEE Transactions on Neural Networks*, *9*(6), 1509-1514.

[8] Hayakawa, T., Hadda, W. M., Hovakimyan, N., & Chellaboina, V. (2005). Neural network adaptive control for nonnegative nonlinear dynamical system. *IEEE Transactions on Neural Networks*, *16*(2), 399-413.

[9] Hung, L. C., Lin, H. P., & Chung, H. Y. (2007a). Design of self-tuning fuzzy sliding mode control for TORA system. *Expert Systems with Applications*, *32*(1), 201-212.

[10] Hung, L. C., & Chung, H. Y. (2007b). Decoupled control using neural network-based sliding-mode controller for nonlinear systems. *Expert Systems with Applications*, *32*(4), 1168-1182.

[11] Hung, S. J., & Hung, K. S. (2001). An adaptive fuzzy sliding-mode controller for servomechanism disturbance rejection. *IEEE Transactions on Industrial Electronics*, *48*(4), 845-852.

[12] Jan, J. C., & Hung, S. L. (2001). High-order MS_CMAC neural network. *IEEE Transactions on Neural Networks*, *12*(3), 598-603.

[13] Lane, S. H., Handelman, D. A., & Gelfand, J. J. (1992). Theory and development of higher-order CMAC neural networks. *IEEE Control Systems Magazine*, *12*(2), 23-30.

[14] Li, H. X., & Tong, S. (2003). A hybrid adaptive fuzzy control for a class of nonlinear MIMO systems. *IEEE Transactions on Fuzzy Systems*, *11*(1), 24-34.

[15] Lin, C. S., & Chiang, C. T. (1998). Integration of CMAC technique and weighted regression for effective learning and output differentiability. *IEEE Transactions on Systems, Man, and Cybernetics, Part B: Cybernetics*, *28*(2), 231-237.

[16] Lin, C. M., & Hsu, C. F. (2002). Guidance laws design by adaptive fuzzy sliding-mode control. *AIAA Journal of Guidance, Control, and Dynamics*, *25*(2), 248-256.

[17] Lin, C. M., & Hsu, C. F. (2003). Neural network hybrid control for antilock braking systems. *IEEE Transactions on Neural Networks*, *14*(2), 351-359.

[18] Lin, C. M., & Hsu, C. F. (2004). Adaptive fuzzy sliding-mode control for induction servomotor systems. *IEEE Transactions on Energy Conversion*, *19*(2), 362-368.

[19] Lin, C. M., & Peng, Y. F. (2004). Adaptive CMAC-based supervisory control for uncertain nonlinear systems. *IEEE Transactions on Systems, Man, and Cybernetics, Part B: Cybernetics*, *34*(2), 1248-1260.

[20] Lin, C. M., Peng, Y. F., & Hsu, C. F. (2004). Robust cerebellar model articulation controller design for unknown nonlinear systems. *IEEE Transactions on Circuits and Systems—Part II: Analog and Digital Signal Processing*, *51*(7), 354-358.

[21] Lin, C. M., & Peng, Y. F. (2005). Missile guidance law design using adaptive cerebellar model articulation controller. *IEEE Transactions on Neural Networks*, *16*(3), 636-644.

[22] Lin, C. K., & Wang, S. D., (2004) An adaptive H^{∞} controller design for bank-to-turn missiles using ridge Gaussian neural networks. *IEEE Transactions on Neural Networks*, *15*(6), 1507-1516.

[23] Salim, L., Mohamed, S. B., & Thierry, M. G. (2005). Adaptive fuzzy control of a class of MIMO nonlinear systems. *Fuzzy Sets and Systems*, *151*(1), 59-77.

[24] Tong, S., Li, H. X., & Chen, G. (2004). Adaptive fuzzy decentralized control for class of large-scale nonlinear systems. *IEEE Transactions on Systems, Man, and Cybernetics, Part B: Cybernetics*, *34*(1), 770-775.

[25] Tong, S., Li, H. X., & Wang, W. (2004). Observer-based adaptive fuzzy control for SISO nonlinear systems. *Fuzzy Sets and Systems*, *148*(3), 355-376.

[26] Wang, C. H., Lin, T. C., Lee, T. T., & Liu, H. L. (2002). Adaptive hybrid intelligent control for uncertain nonlinear dynamical systems. *IEEE Transactions on Systems, Man, and Cybernetics, Part B: Cybernetics*, *32*(5), 583-597.

[27] Wang, L. X. (1994). *Adaptive fuzzy systems and control: design and stability analysis.* Prentice-Hall, Englewood Cliffs, NJ.